PROCEEDINGS OF SCIENCE

Overview of CKM metrology from semileptonic B decays

Stefano Moneta[a,b,*]

[a] *INFN Sezione di Perugia, I-0612 3 Perugia, Italy*

[b] *Dipartimento di Fisica, Università di Perugia, I-06123 Perugia, Italy*

E-mail: stefano.moneta@pg.infn.it

The determination of the CKM matrix elements $|V_{ub}|$ and $|V_{cb}|$ from semileptonic B decays is fundamental to improve the existing constraint on the unitary triangle. The experimental measurements, however, show some inconsistencies depending on the reconstruction approach (inclusive or exclusive) of the hadronic final states. Further experimental inputs are therefore needed to understand their origin. The Belle II experiment has just begun to provide a variety of different measurements which in the next years will be competitive with the world averages. Similarly, the LHCb experiment can deliver complementary results exploiting b-baryons and B_s mesons. In the following, some of the relevant results obtained with the first dataset collected at the Belle II experiment and the Run-1 dataset of the LHCb experiment are briefly outlined.

Workshop Italiano sulla Fisica ad Alta Intensità (WIFAI2023)
8-10 November 2023
Dipartimento di Architettura dell'Università Roma Tre, Rome, Italy

*Speaker

© Copyright owned by the author(s) under the terms of the Creative Commons Attribution-NonCommercial-NoDerivatives 4.0 International License (CC BY-NC-ND 4.0).

PoS(WIFAI2023)003

1. Introduction

Flavor physics, and in particular the phenomena involving b quarks, has raised increasing interest in the last decade because of the observation of several deviations from Standard Mode (SM) expectations. High precision measurements of b quark decays can provide an indirect test to physics beyond the SM, probing energy scales not directly reachable with the existing particle colliders.

Semileptonic B decays are tree-level processes in the SM, involving a charged-current transition of a b quark to an up-type quark, together with a $W \to \ell\nu$ emission. These processes are well-understood from a theoretical point of view, and the precision of the calculation is mainly limited by the hadronic form factors uncertainties. Furthermore, the amplitude of a semileptonic $b \to x$ process depends on the CKM matrix element V_{xb}, hence the module of V_{xb} can be extracted from the measurement of the decay rate. A precise determination of $|V_{ub}|$ and $|V_{cb}|$ is nowadays particularly important to improve theoretical constraints on the CKM unitary triangle, as well as the predictions of rare decays such as $K \to \pi\nu\overline{\nu}$ and $B \to \tau\nu$, possibly sensitive to new physics models.

In general, two complementary approaches are considered for semileptonic decays, depending on whether the hadronic final states are inclusively or exclusively reconstructed. The exclusive measurement targets specific hadronic final states, while in the inclusive reconstruction all the possible final states containing an u or c quark are included altogether. The inclusive measurement, though experimentally more challenging, does not need to rely on the hadronic form factors estimation from theory, which is a major source of uncertainties in the exclusive approach. The current world average $|V_{xb}|$ measurements present a discrepancy of about 3.3 σ between inclusive and exclusive determinations for both $|V_{ub}|$ and $|V_{cb}|$ [1]. As far as today, this tension is not explained, although it may originate from a mis-modeling of the form factors. Such discrepancy limits the precision of $|V_{ub}|$ and $|V_{cb}|$, and calls for inputs from both theory and experiment.

2. $|V_{xb}|$ measurements at Belle II

The Belle II experiment, located at the SuperKEKB electron-positron collider in Japan, has collected a total integrated luminosity of 364 fb^{-1} at the $B\overline{B}$ pair production threshold ($\Upsilon(4S)$ resonance) in the 2019-2022 period. The Belle II detector [2] is a cylindrical spectrometer with a tracking system, Cherenkov detectors dedicated to particle identification, an electromagnetic calorimeter, and an outermost detector to identify muons and K_L. Thanks to the high hermeticity of the detector, the missing neutrino in $e^+e^- \to B\overline{B}$ events, where one B decays semileptonically, can be indirectly reconstructed.

A semileptonic B decay in a $e^+e^- \to B\overline{B}$ event can be identified either by reconstructing the partner B in a fully hadronic decay and isolating the semileptonic B (tagged approach), or by directly looking for a semileptonic final state, ignoring the other B meson decay (un-tagged approach). The advantage of the tagged method is that the kinematic of the event can be fully closed, allowing to estimate the flight direction of the neutrino and to reject backgrounds from mis-reconstructed B mesons, particularly helpful for inclusive

PoS(WIFAI2023)003

measurements. However, the signal efficiency is much lower with respect to the un-tagged method, as it depends on the hadronic B tagging efficiency, which is about 0.4% for the Full Event Interpretation algorithm developed at the Belle II experiment [3]. Furthermore, the calibration of the B tagging algorithm is an additional systematics for the tagged approach, hence for exclusive measurements the un-tagged method is in general preferred.

2.1 $|V_{cb}|$ measurement from $B^0 \to D^{*-}\ell^+\nu$ decay

An exclusive determination of $|V_{cb}|$ was performed using 189 fb^{-1} of Belle II data and exploiting the semileptonic decay $B^0 \to D^{*-}\ell^+\nu$, where ℓ can be both an electron or a muon (charge conjugates are hereafter implied). Both the un-tagged [4] and tagged [5] approaches are carried on in two distinct analyses.

The D^{*-} resonance is reconstructed as $D^{*-} \to D^0\pi^-$, whose flavor is identified by the charge of the lowest momentum pion. $B^0 \to D^{*-}(\to D^0\pi^-)\ell^+\nu$ kinematics can be fully parameterized with three helicity angles θ_ℓ, θ_V, χ and a recoil parameter w. Here θ_ℓ is the angle between the direction of the lepton and of the B^0 meson in the W rest frame; θ_V is the angle between the direction of the D^0 and the B^0 in the D^{*-} vector reference frame; χ is the angle formed by the decay planes of the W and the D^{*-} in the B^0 rest frame. The recoil parameter w is defined as the product of the B^0 and D^{*-} four-velocities. Exploiting these parameters, the fully differential decay rate can be written as:

$$\frac{d\Gamma(B^0 \to D^{*-}\ell^+\nu)}{dw\, d\cos\theta_\ell\, d\cos\theta_V\, d\chi} \propto |V_{cb}|^2\, |\mathcal{F}(w,\, \cos\theta_\ell,\, \cos\theta_V,\, \chi)|^2 \tag{1}$$

where $\mathcal{F}$ is the theoretical differential form factor for $B^0 \to D^{*-}$.

2.1.1 Un-tagged $B^0 \to D^{*-}\ell^+\nu$

The main challenge for an un-tagged differential measurement of the branching ratio is the reconstruction of the B^0 flight direction. The semileptonic decay can be treated as a two-body $B^0 \to Y\nu$ decay, into a visible $Y = D^{*-}\ell^+$ system and an invisible neutrino. The direction of the B^0 momentum is then constrained on the surface of a cone around the Y momentum direction and with opening angle θ_{BY}, determined by the measured Y four-momentum and the known center of mass energy of the B^0 meson. In order to estimate the direction of the B^0 on the cone, the information of the $\Upsilon(4S) \to B\overline{B}$ polarization is combined with the information from all the tracks and calorimeter clusters in the event not associated to the semileptonic B [6, 7]. For a signal event, neglecting beam-induced background, such remaining objects are expected to come from solely from the partner B meson, hence their total momentum is correlated to the B flight direction. This method leads to a significant improvement in the resolution of all the θ_ℓ, θ_V, χ, and w parameters, with respect to the previous methods adopted by Belle and BaBar.

Once all the kinematic parameters are reconstructed, the signal yield is extracted in each bin of w, $\cos\theta_\ell$, $\cos\theta_V$ and χ through a two-dimensional fit on $\cos\theta_{BY}$, which for signal events should stay between -1 and $+1$, and on the difference ΔM between the reconstructed D^{*-} mass and the D^0 mass, which can separate the peaking real D^* events

PoS(WIFAI2023)003

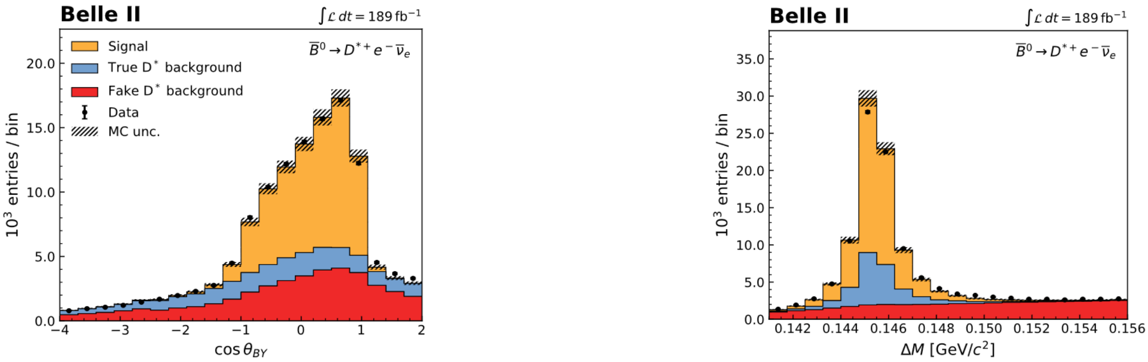

Figure 1: Distributions of the reconstructed $\cos\theta_{BY}$ (left) and $\Delta M = M(D^{*-}) - M(D^0)$ (right) distributions exploited for fitting the signal yield in the un-tagged $B^0 \to D^{*-}\ell^+\nu$ analysis. Both data and simulation are shown with their respective uncertainties.

from combinatorial backgrounds. The distributions of the fitting variables for data and simulation are shown in Figure 1.

The value of $|V_{cb}|$ is finally derived via a simultaneous fit of the extracted signal in bins of the four kinematic variables. The BGL model [8] is exploited for form factors parameterization, including lattice QCD inputs in the zero-recoil region [10]. The fitted $|V_{cb}|$ value is:

$$|V_{cb}|_{\mathrm{BGL}} = (40.57 \pm 0.31 \pm 0.95 \pm 0.58) \times 10^{-3}$$

where the uncertainties are, in order, statistical, systematics, and from the theoretical model. A compatible result is obtained using the alternative CLN [9] form factor parameterization. The dominant source of systematic uncertainty is the calibration of the slow pion efficiency for reconstructing the $D^{*-} \to D^0\pi^-$. The result is compatible with both inclusive and exclusive HFLAV averages of $|V_{cb}|$.

2.1.2 Tagged $B^0 \to D^{*-}\ell^+\nu$

In the tagged approach, the B^0 flight direction is estimated from the reconstructed momentum of the hadronic tagged B meson, which in the center of mass frame is opposite to the momentum of the semileptonic B^0. The signal yield is extracted through a fit on the missing mass squared distribution, defined as the square of the missing four-momentum in the event: $m^2_{\mathrm{miss}} = (P_{\mathrm{beam}} - P_{B_{\mathrm{tag}}} - P_{D^*} - P_\ell)^2$. For signal events such variable is peaked at the neutrino mass, as shown in the left plot of Figure 2.

Since the signal efficiency is much lower than for the un-tagged approach, in this case, the decay rate is differentiated only in the recoil parameter w. The value of $|V_{cb}|$ is then fitted from the extracted signal decay rate in 10 bins of w (right plot of Figure 2) using the CLN parameterization of the form factors:

$$|V_{cb}|_{\mathrm{CLN}} = (37.9 \pm 2.7) \times 10^{-3}$$

PoS(WIFAI2023)003

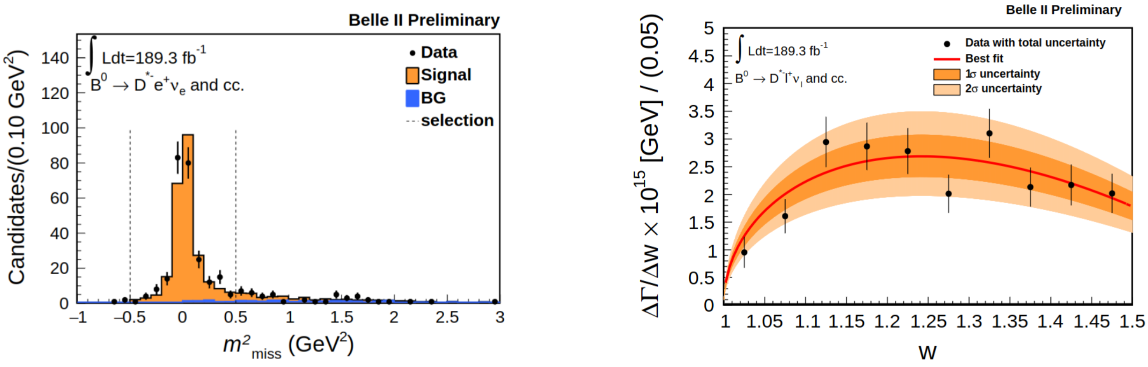

Figure 2: Distribution of the missing mass squared used for extracting the signal yield in the hadronic tagged $B^0 \to D^{*-}\ell^+\nu$ analysis (left plot). $B^0 \to D^{*-}\ell^+\nu$ decay rate in bins of recoil parameter w, fitted by the CLN form factor model in the tagged analysis (right plot).

where the uncertainty is dominated by the systematics, and the dominant sources derive from the calibration of the B tagging algorithm and of the slow pion efficiency.

2.2 $|V_{ub}|$ measurement from un-tagged $B^0 \to \pi^-\ell^+\nu$ decay

The first determination of $|V_{ub}|$ at the Belle II experiment is performed in the exclusive semileptonic decay $B^0 \to \pi^-\ell^+\nu$, with an un-tagged approach, using 189 fb^{-1} of data [11]. As for exclusive $|V_{cb}|$, $|V_{ub}|$ is also extracted from a fit to the differential decay rate, in this case in bins of the momentum transfer squared $q^2 = (P_B - P_\pi)^2$. The B^0 momentum direction is estimated again constraining the cone surface around the momentum of the $\pi^-\ell^+$ system and combining the information from the remaining objects in the event with the angular distribution of a $\Upsilon(4S)$ decay.

The signal yield is then extracted in six bins of q^2, with a simultaneous fit on two extraction variables, capable of separating events where the B^0 energy and momentum are correctly estimated from mis-reconstructed events. The energy difference ΔE between the reconstructed B^0 meson in the center of mass frame and the beam energy, which is expected to peak at zero for the signal (left plot of Figure 3). The beam-constrained mass $M_{bc} = \sqrt{E^{*2}_{\mathrm{beam}} - |\vec{p}_B|^2}$, i.e. the invariant mass of the reconstructed B assuming its energy equal to the beam energy, peaks at 5.29 GeV$/c^2$ for the signal candidates (right plot of Figure 3). The $|V_{ub}|$ value is finally fitted from the extracted q^2 spectrum of the $B^0 \to \pi^-\ell^+\nu$ decay rate and using the form factors parameterization derived from lattice QCD [12]:

$$|V_{ub}| = (3.55 \pm 0.12 \pm 0.13 \pm 0.17) \times 10^{-3}$$

where the uncertainties are, in order, statistical, systematic, and theoretical. The limiting systematic source arises from the modeling of the continuum light quarks $e^+e^- \to q\bar{q}$ backgrounds, which are validated on a control sample of data collected 60 MeV below the $B\overline{B}$ production threshold, whose size is limited to 18 fb^{-1}. The central value is in agreement with the HFLAV average of the previous exclusive $|V_{ub}|$ measurements.

PoS(WIFAI2023)003

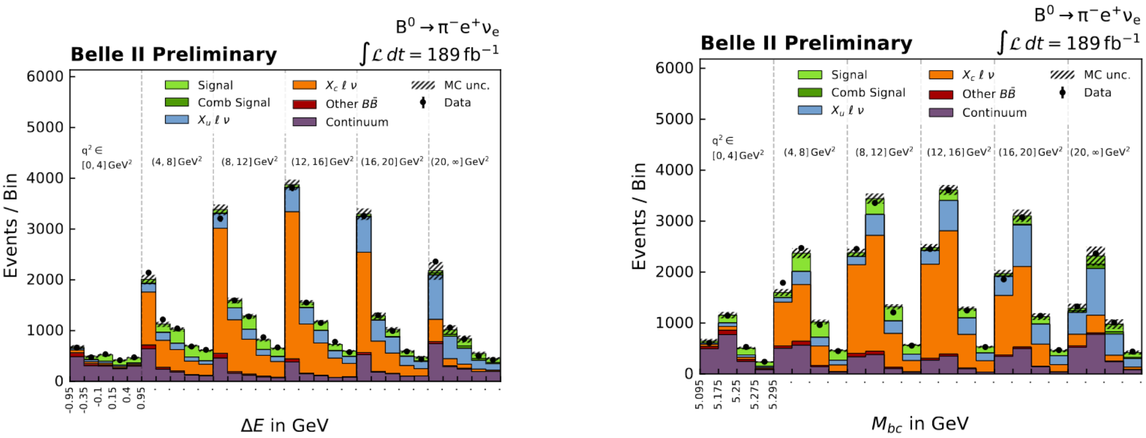

Figure 3: Distributions of the energy difference ΔE (left) and beam constrained mass M_{bc} (right) used for the extraction of the signal yield in the $B^0 \to \pi^- \ell^+ \nu$ un-tagged analysis.

3. $|V_{xb}|$ measurements at LHCb

The LHCb experiment, located at the LHC hadron collider, consists of a single-arm forward spectrometer covering the pseudorapidity range $2 < \eta < 5$ [13]. The excellent vertex capabilities of the LHCb detector allow to reconstruct the flight direction of b hadrons produced in pp collisions, making possible to recover the kinematics in case of semi-leptonic decays with a single missing neutrino. LHCb can therefore compete with B factories on the exclusive determination of $|V_{ub}|$ and $|V_{cb}|$ elements.

3.0.1 Determination of $|V_{ub}|/|V_{cb}|$ from $B_s^0 \to K^- \mu^+ \nu$

Exploiting the Run-1 dataset, corresponding to 2 fb^{-1} collected at $\sqrt{s} = 8$ TeV, LHCb has determined the ratio $|V_{ub}|/|V_{cb}|$ from semi-leptonic decays $B_s^0 \to K^- \mu^+ \nu$ and $B_s^0 \to D_s^- \mu^+ \nu$ [14]. Thanks to the presence of a heavier spectator quark, the B_s mesons are considered theoretically cleaner with respect to B^+ and B^0.

The B_s mass is represented by the corrected mass $m_{\mathrm{corr}} = \sqrt{m_{X\mu}^2 + p_\perp^2} + p_\perp$, where $X\mu$ is the system of visible final states ($X = K^-$ or $X = D_s^-$), and $p_\perp$ is the momentum orthogonal to the B_s flight direction, reconstructed from the primary and secondary vertices. The $B_s^0 \to K^- \mu^+ \nu$ signal yield N_K is extracted from a fit on the m_{corr} distribution into two different q^2 regions, below and above 7 GeV$^2/c^4$, shown in the left and right plots of Figure 4, respectively. On the other hand, the normalization channel $B_s^0 \to D_s^- \mu^+ \nu$ is reconstructed by targeting a $D_s^- \to K^+ K^- \pi^-$ candidate. The yield N_{D_s} of $B_s^0 \to D_s^- \mu^+ \nu$ events is determined through a simultaneous fit of the D_s^- invariant mass distribution and of the m_{corr} distribution.

The efficiencies ϵ_K for $B_s^0 \to K^- \mu^+ \nu$ and ϵ_{D_s} for $B_s^0 \to D_s^- \mu^+ \nu$ are both extracted from simulation, applying data-driven corrections to account for possible mismodeling. The ratio of branching fractions is then determined as:

PoS(WIFAI2023)003

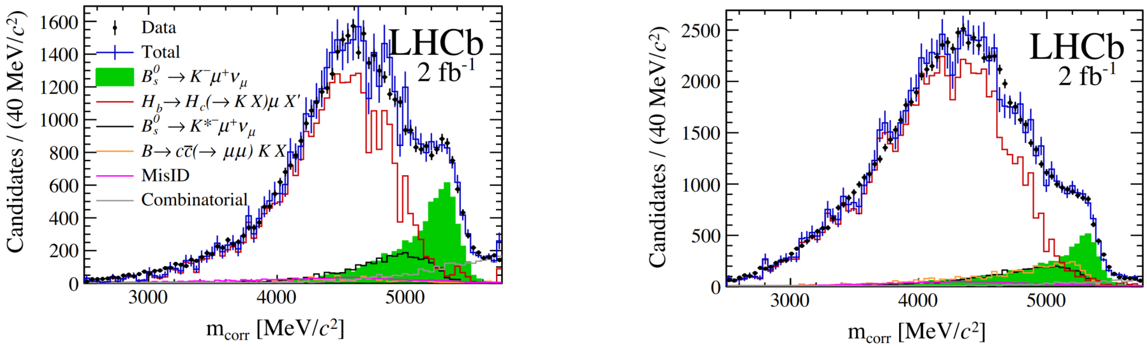

Figure 4: Distribution of the corrected mass $m_{\rm corr}$ of reconstructed $B_s^0 \to K^- \mu^+ \nu$ decays for $q^2 < 7$ GeV$^2/c^4$ (left plot) and $q^2 > 7$ GeV$^2/c^4$ (right plot).

$$R_{\rm BF} \equiv \frac{\mathcal{B}(B_s^0 \to K^- \mu^+ \nu)}{\mathcal{B}(B_s^0 \to D_s^- \mu^+ \nu)} = \frac{N_K}{N_{D_s}} \frac{\epsilon_{D_s}}{\epsilon_K} \times \mathcal{B}(D_s^- \to K^+ K^- \pi^-)$$

where the branching ratio of $D_s^- \to K^+ K^- \pi^-$ decay is taken as an external measurement [15]. The ratio of CKM matrix elements is extracted from the relation $R_{\rm BF} = |V_{ub}|^2/|V_{cb}|^2 \times$ FF$_K$/FF$_{D_s}$, where the form factor prediction from LQCD is used in the high q^2 region, while the LCSR calculation is adopted for the low q^2 interval, resulting in $|V_{ub}|/|V_{cb}| = 0.061 \pm 0.004$ and $|V_{ub}|/|V_{cb}| = 0.095 \pm 0.008$, respectively for the low and the high q^2 regions. The uncertainties are dominated by the form factors knowledge, which are driving the discrepancy between the two q^2 regions.

4. Conclusion

The long-standing puzzle of the discrepancy between inclusive and exclusive measurements is still present and new inputs from both theory and experiments are needed to understand its origin. With the upcoming increase in the size of the data sample, Belle II is expected to play a major role in the determination of $|V_{xb}|$ elements from semileptonic B decays, being able to access both exclusive and inclusive channels. The un-tagged method has higher statistical power, though a lower purity, compared to the tagged one, which is limited by statistics and has an additional systematic uncertainty from the calibration of the B tagging algorithm. A better understanding of the detector will allow to reduce all the main systematic sources on the future measurements, reaching a 1% precision in the overall $|V_{cb}|$ determination and at least 3% in both inclusive and exclusive $|V_{ub}|$ [16]. In the meantime, LHCb is expected to provide complementary measurements with the increased statistics from Run-2 and Run-3 datasets, focusing in particular on the exclusive $|V_{xb}|$ determination, and exploiting the production of B_s mesons and b baryons.

References

[1] Y. Amhis et al. (HFLAV) "Averages of b-hadron, c-hadron, and τ-lepton properties as of 2021". In: *Phys. Rev. D* 107, 2470-0029 (2023).

PoS(WIFAI2023)003

[2] T. Abe et al. “Belle II Technical Design Report”. In: arXiv:1011.0352 (2010).

[3] T. Keck et al. “The Full Event Interpretation”. In: *Computing and Software for Big Science* 3.1 (2019).

[4] I. Adachi et al. (Belle II Collaboration) “Determination of $|V_{cb}|$ using $\overline{B}^0 \to D^{*+}\ell^-\overline{\nu}_\ell$ decays with Belle II”. In: *Phys. Rev. D* 108, 092013 (2023).

[5] F. Abudinén et al. (Belle II Collaboration) “Measurement of the $B^0 \to D^{*-}\ell^+\nu_\ell$ branching ratio and $|V_{cb}|$ with a fully reconstructed accompanying B meson in 2019-2021 Belle II data”. In: arXiv:2301.04716 (2023).

[6] B. Aubert et al. “Measurements of the $B \to D^*$ form factors using the decay $\overline{B}^0 \to D^{*+}e^-\overline{\nu}_e$”. In: *Phys. Rev. D* 74, 092004 (2006).

[7] E. Waheed et al. “Measurement of the CKM Matrix Element $|V_{cb}|$ from $B0 \to D^{*-}\ell^+\nu_\ell$ at Belle”. In: *Phys. Rev. D* 100, 052007 (2019).

[8] C. G. Boyd, B. Grinstein, and R. F. Lebed “Precision corrections to dispersive bounds on form factors”. In: *Phys. Rev. D* 56, 6895 (1997).

[9] I. Caprini, L. Lellouch, and M. Neubert “Dispersive bounds on the shape of $B \to D^*\ell\nu$ form factors”. In: *Nucl. Phys. B* 530, pp. 153-181 (1998).

[10] J. A. Bailey et al. (Fermilab Lattice and MILC Collaborations) “Update of $|V_{cb}|$ from the $\overline{B} \to D^*\ell\nu$ form factor at zero recoil with three-flavor lattice QCD”. In: *Phys. Rev. D* 89, 114504 (2014).

[11] K. Adamczyk et al. (Belle II Collaboration) “Determination of $|V_{ub}|$ from untagged $B^0 \to \pi^-\ell^+\nu_\ell$ decays using 2019-2021 Belle II data”. In: arXiv:2210.04224 (2022).

[12] J. A. Bailey et al. (Fermilab Lattice and MILC Collaborations) “$|V_{ub}|$ from $B \to \pi\nu$ decays and $(2+1)$-flavor lattice QCD”. In: *Phys. Rev. D* 92, 014024 (2015).

[13] A. A. Alves Jr. et al. (LHCb Collaboration), “The LHCb detector at the LHC”. In: *J. Instrum.* 3, S08005 (2008).

[14] R. Aaij et al. (LHCb Collaboration) “First Observation of the Decay $B_s^0 \to K^-\mu^+\nu_\mu$ and a Measurement of $|V_{ub}|/|V_{cb}|$”. In: *Phys. Rev. Lett.* 126, 081804 (2021).

[15] P. A. Zyla et al. (Particle Data Group), “Review of particle physics”. *Prog. Theor. Exp. Phys.*, 083C01 (2020).

[16] L. Aggarwal et al. “Snowmass White Paper: Belle II physics reach and plans for the next decade and beyond”. In: arXiv:2207.06307 (2022).

PoS(WIFAI2023)003